3-D Numerical simulation of ceramic breeder blanket pebble bed thermomechanics - methodology and preliminary results

Z. Lu, A.Y. Ying and M.A. Abdou

Mechanical and Aerospace Engineering Department, University of California, Los Angeles, Los Angeles, CA 90095-1597

Abstract

A new 3-D numerical model is underdevelopment to simulate particle bed thermomechanical behavior. The evolution of the particle-particle contact characteristics under internal (simulating thermal expansion and radiation swelling) and external loading can be monitored while its subsequent impact on bed heat transfer characteristics and temperature profile can be better quantified. In this paper, mathematical formulation as well as model predictions on the particle bed thermomechanical states under imposed and induced strains are presented. Preliminary simulations are performed to understand stress-strain relationship in response to the uniaxial and hydrostatic pressure loads. The results of the calculated bed effective modulus compares reasonably well with the experimental data.

1. Introduction

Particulate materials in the form of particle bed have been considered for shielding and tritium breeding as well as neutron multiplication in many of the conceptual fusion reactor blanket designs. The thermal and mechanical properties of particle bed directly affect the blanket thermomechanical performance. Those include effective modulus and coefficient of thermal expansion, effective thermal conductivity, inter-particle conductance, and particle bed-wall conductance. Substantial experimental and modeling efforts have been carried out to characterize the thermal and mechanical properties of ceramic breeder blanket materials [1-3]. Those results provided preliminary information regarding the order of the magnitude in terms of effective modulus and the overall stresses.

Experimentally it is difficult to quantify the thermal and mechanical properties of particulate materials in details and precisely, especially for the blanket designs in which particle beds are used. Also the discrete nature of the particulate materials is very difficult to describe, based only on the macroscopic behaviors. Discrete numerical simulations, used in a proper way and checked by experiments, are more flexible in their application and can provide essentially any desired piece of information (stress, strain, and detailed micro-mechanical statistics and spatial distributions of particles at any time) that is not available in real physical experiments.

The distinct element method (DEM) developed by Cundall [4,5] has been successfully applied to analyses of granular assemblies. The fundamental idea of the method is based on the Newton's

second law and problems are treated as dynamical ones. DEM is highly effective in case of rapid granular flow or time-dependent processes. But its disadvantages appear when equilibrium is needed—Displacements are usually over-estimated and the calculated state oscillates around the exact solution. Kishino [6] published a model similarly to DEM; the algorithm calculates the displacements of each grain independently of the others, but the grains are displaced according to stiffness of the contacts with neighboring elements. Large displacements and rearrangements can easily be followed but it has slow convergence—even if the displacements are small and structure of the assembly does change, many iteration cycles are necessary. Serrano and Rodriguez-Oritiz [7] built a quasi-static model based on the compilation of global stiffness matrix. This method has the disadvantage of major computational effort on rearranging and reformulating the global stiffness matrix for the contacts, whenever any new contact is formed or an old one disappears.

In this paper, a different 3D numerical model is presented to simulate the thermal and mechanical properties of particle bed. It is a quasi-static model and no time-effects are considered. The particle bed is modeled as a collection of rigid particles interacting via Hertz type contact force [8-10]. A 3D isotropic spring simulates particle-environment relation; then the incremental displacement of each particle can be calculated based on Hooke's law. Preliminary simulations are performed to understand particle bed stress-strain relationship in response to the uniaxial and hydrostatic pressure loads.

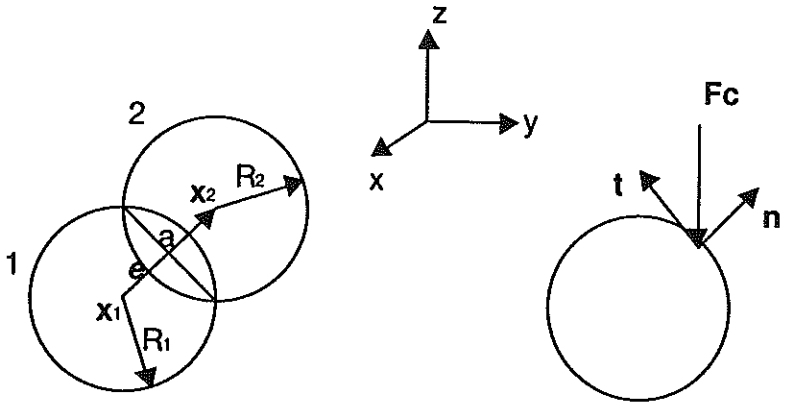

Figure 1. Contact between two particles

2. Numerical model

Interface normal contact force

The normal contact force law is presented for the case of two spheres in contact, sphere 1 and sphere 2 in Figure 1. The usual tensor notation in the Cartesian coordinate system is adopted. The coordination of the sphere centers are represented as x_1 (x_1, y_1, z_1) and x_2 (x_2, y_2, z_2) where indices x, y, and z refer to the coordination of a Cartesian coordinate system as indicated in Figure 1. The

detection of contacts between two particles is done in a straightforward fashion, where the radii of two vicinity particles are checked for overlap. If spheres 1 and 2 have radii R_1 and R_2, they are taken to be in contact only if the distance D between their centers is less than the sum of their radii

$$D < R_1 + R_2 \tag{1}$$

and

$$D = \sqrt{(x_1 - x_2)^2 + (y_1 - y_2)^2 + (z_3 - z_3)^2} \tag{2}$$

The unit vector e=(cosα, cosβ, cosγ) (see Figure 1) is introduced as pointing from the center of sphere 1 to the center of sphere 2, i.e.

$$\mathbf{e} = \frac{\mathbf{x}_1 - \mathbf{x}_2}{D} = (\cos\alpha, \quad \cos\beta, \quad \cos\gamma) \tag{3}$$

The relative approach of the particles in contact is obtained in terms of the diameter of the contact area, a, the normal force at the interface, F_n, and the elastic properties of the particles. The resultant normal contact force F_n is expressed by [8]

$$F_n = \frac{4E^*\sqrt{R\delta^3}}{3} \tag{4}$$

where

$$\delta = R_1 + R_2 - D, \qquad \delta = \frac{a^2}{4R} \tag{5}$$

$$\frac{1}{E^*} = \frac{1-\nu_1^2}{E_1} + \frac{1-\nu_2^2}{E_2} \tag{6}$$

$$\frac{1}{R} = \frac{1}{R_1} + \frac{1}{R_2} \tag{7}$$

R is the relative curvature, E_1 and E_2 are the Young's moduli, ν_1 and ν_2 are the Poisson's ratios, R_1 and R_2 are the radii of the particles in contact, respectively.

Interface tangential friction force

The friction at an interface has been traditionally described using Coulomb's friction law that states that at incipient sliding, the friction force is given by

$$F_f = F_n \tan\phi_\mu \tag{8}$$

where ϕ_μ is the interface friction angle. Although microscopic processes associated with interface friction are being explored, the interface friction phenomenon has not been completely understood [11]. In light of this, Coulomb's friction law and friction angle are used in this work.

Particle motion law

First the force-displacement law will be developed for 2D case and then it will be extended to the 3D situation. If only considering the normal contact force, the contact force F_c reduces to normal contact force F_n. The x, y, and z components of the contact force F_c acted at the contact point c are denoted as F_{xc}, F_{yc}, and F_{zc}, then

$$F_c = \begin{pmatrix} F_{xc} \\ F_{yc} \\ F_{zc} \end{pmatrix} = \begin{pmatrix} F_n \cos\alpha \\ F_n \cos\beta \\ F_n \cos\gamma \end{pmatrix} \tag{9}$$

Under quasi-static conditions the inertial forces may be neglected and the equation of motion reduces to the following equilibrium conditions

$$F - \sum_c F_c = 0 \tag{10}$$

where F are the externally imposed force and the summation $\sum_c$ is performed over the contacts of the particle. Each particle in the assembly should satisfy the above equilibrium equation.

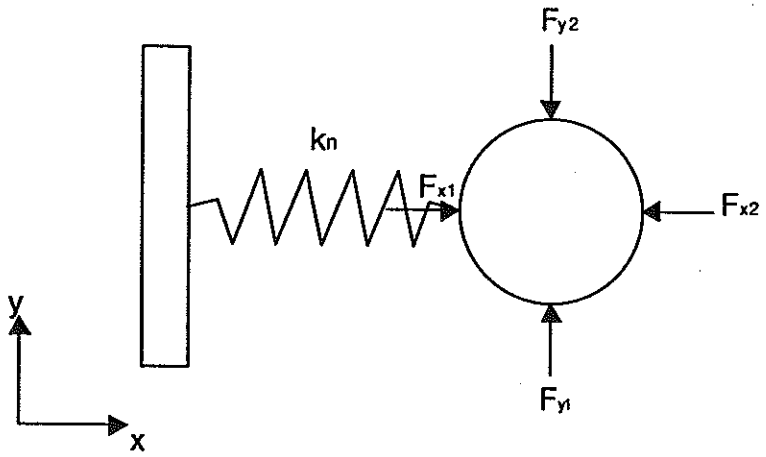

Figure 2. Equivalent forces exerted on a particle

Considering a single particle connected to external environment through a spring as indicated in Figure 2, except the spring force, the total force in x direction is

$$F_x = F_{x1} - F_{x2} - k_f (F_{y1} + F_{y2}) \tag{11}$$

where k_f=tanϕ_μ is the friction coefficient, F_{x1}, F_{x2} and F_{y1}, F_{y2} are the total positive and negative normal contact forces in x, y directions respectively. If the normal contact forces at all contact points of the particle have been calculated through (4), then

$$F_{x1} - F_{x2} = \sum_c F_{xc} \tag{12}$$

$$F_{y1} + F_{y2} = \sum_c |F_{yc}| \tag{13}$$

Σ_c represents the summation over the contact points of the particle. If the spring stiffness is k_n, then the incremental displacement of the particle in x direction is given by Hooke's law as

$$\Delta D_x = \frac{F_x}{k_n} = \frac{\sum_c F_{xc} \pm k_f \sum_c |F_{yc}|}{k_n} \tag{14}$$

$$for \quad |\sum_c F_{xc}| > k_f \sum_c |F_{yc}| \quad otherwise$$

$$\Delta D_x = 0$$

Since the friction force is always at the direction that is opposite to the particle motion direction, the ± sign in the equation (14) should be chosen such that the friction force is opposite to the active force ($\Sigma_c F_{xc}$). Similarly the incremental displacement in y direction is

$$\Delta D_y = \frac{F_y}{k_n} = \frac{\sum_c F_{yc} \pm k_f \sum_c |F_{xc}|}{k_n} \tag{15}$$

$$for \quad |\sum_c F_{yc}| > k_f \sum_c |F_{xc}| \quad otherwise$$

$$\Delta D_y = 0$$

Here the particle is supposed to connect to the environment through a 2D isotropic spring of stiffness k_n. For three-dimension, similarly to 2D situation, the particle is assumed connect to the outside environment through a 3D isotropic spring of stiffness k_n. And the incremental displacement of the particle is given by

$$\Delta D_x = \frac{F_x}{k_n} = \frac{\sum_c F_{xc} \pm k_f \sqrt{(\sum_c |F_{yc}|)^2 + (\sum_c |F_{zc}|)^2}}{k_n} \qquad (16)$$

for $\left| \sum_c F_{xc} \right| > k_f \sqrt{(\sum_c |F_{yc}|)^2 + (\sum_c |F_{zc}|)^2}$ *otherwise*

$$\Delta D_x = 0$$

and

$$\Delta D_y = \frac{F_y}{k_n} = \frac{\sum_c F_{yc} \pm k_f \sqrt{(\sum_c |F_{zc}|)^2 + (\sum_c |F_{xc}|)^2}}{k_n} \qquad (17)$$

for $\left| \sum_c F_{yc} \right| > k_f \sqrt{(\sum_c |F_{zc}|)^2 + (\sum_c |F_{xc}|)^2}$ *otherwise*

$$\Delta D_y = 0$$

and

$$\Delta D_z = \frac{F_z}{k_n} = \frac{\sum_c F_{zc} \pm k_f \sqrt{(\sum_c |F_{xc}|)^2 + (\sum_c |F_{yc}|)^2}}{k_n} \qquad (18)$$

for $\left| \sum_c F_{zc} \right| > k_f \sqrt{(\sum_c |F_{xc}|)^2 + (\sum_c |F_{yc}|)^2}$ *otherwise*

$$\Delta D_z = 0$$

Similarly, the ± signs in equations (16-18) should be chosen such that the friction forces are opposite to the active force. The displacement of each particle is calculated based on the above three equations. Since any displacement of the neighboring contact particles would generate a new non-equilibrium situation, an iterative calculation of successive releasing of forces exerted on a single particle is performed until the resultant force on each particle in the assembly is sufficiently small (Figure 3).

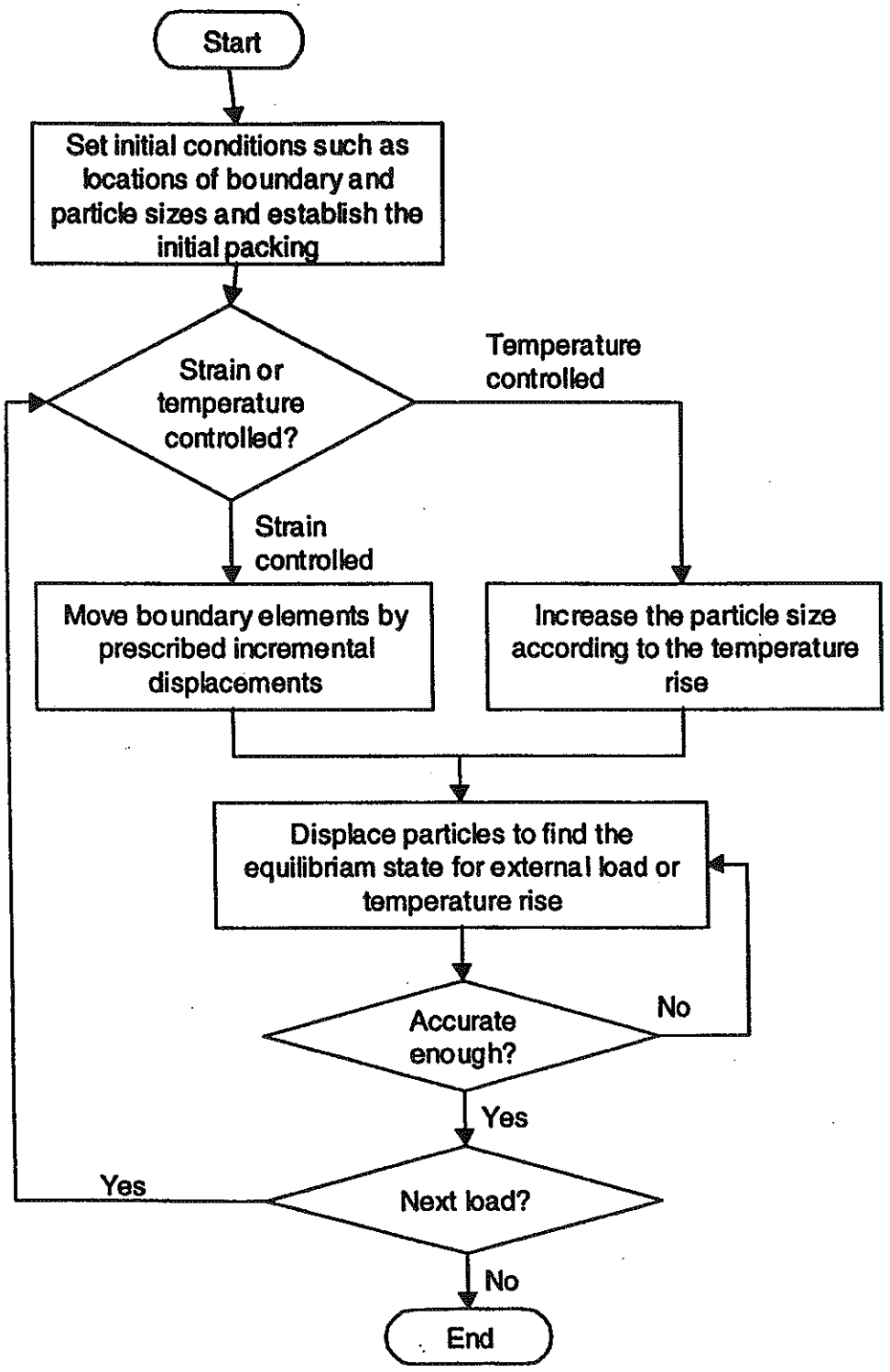

Figure 3: Flow chart of anlysis

Relaxation isotropic spring stiffness k_n

In equations (16)-(18), the stiffness k_n of the relaxation isotropic spring still needs to be determined. k_n is related to the normal contact force for two touching particles in equation (4). Using a linear relationship to approximate the non-linear relationship, i.e., suppose

$$F = k_n \delta \tag{19}$$

To best approximate the equation (4), the least-square regression method is used. The square difference between (4) and (19) is

$$\Delta = \int_0^{\delta_f} \left(\frac{4E^* \sqrt{R\delta^3}}{3} - k_n \delta \right)^2 d\delta \tag{20}$$

To find the value of k_n that Δ is the smallest, let $\partial\Delta/\partial k_n=0$, then

$$k_n = \frac{8E^* \sqrt{R\delta_f}}{7} \tag{21}$$

where δ_f is the average of all the δ_c at particle contact points.

Initial packing assembly

The initial packing assembly is created by a random number generator. As input data, the total particle number and the thermal and mechanical properties of solid particulate material are given, as well as the parameter that controls the particle size range. The size of assembly volume, the minimal and maximal particle radius can be calculated or recorded during the assembly automatic generation process. Then the program searches for an equilibrium state of the assembly. As a result, an assembly consisting of touching particles in equilibrium is obtained.

3. Simulation results

The assembly, including a total of 1000 particles, is assumed to be bounded by six rigid walls that form a cubic volume. The loading is controlled by strain or moving the boundary elements according to the corresponding strain. In the test, the boundary elements are moved symmetrically with respect to the central axes of particle assembly. The stresses are calculated after the equilibrium of assembly is reached; depending on the procedure, next load and corresponding stresses may be taken and calculated.

The calculated result of the average wall stress as a function of compressive strain is illustrated in Figure 4 and Figure 5 for hydrostatic (triaxial) and uniaxial compressions, respectively. The stress-strain responses, in terms of principal stress versus principal strain, are almost linear. The calculated elastic Young's modulus is much smaller than that of solid material, which is consistent with predictions [12] and previous experiment results [1]. Sudden changes in the curve gradient are due to local collapse of the fabric in particle assembly. It seems that local changes in fabric are significant even if in small model. The deformation of the particle bed is a consequence of the displacements of the particles and is irreversible, which indicate the change of state and make it imperative to define the mechanical behavior on the basis of state quantities.

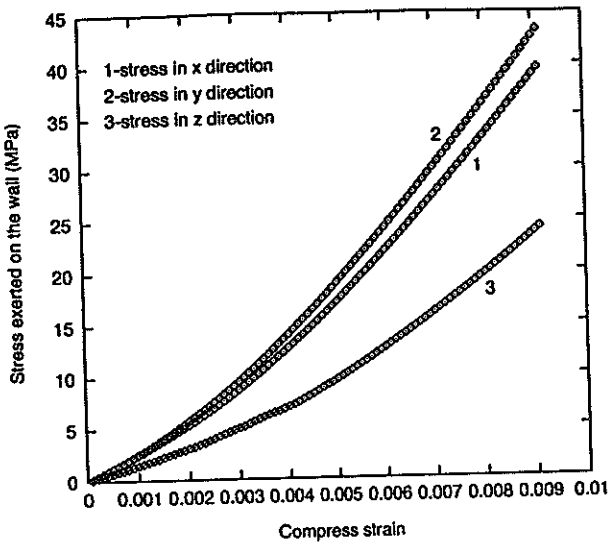

Figure 4 Stress-strain relationship for hydrostatic compression

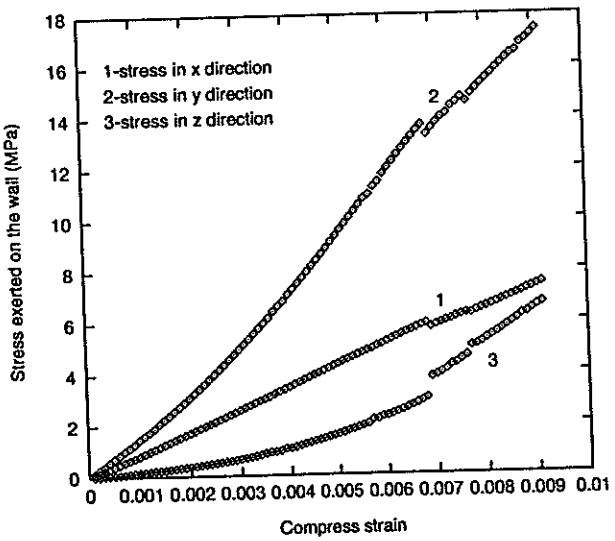

Figure 5 Stress-strain relationship for uniaxial compression

The thermal and mechanical properties can be derived based on the macroscopic state of the bed assembly. From the stress-strain relationship (Hooke's law)

$$\varepsilon_x = \frac{1}{E_p}[\sigma_x - \nu_p(\sigma_y + \sigma_z)] \tag{22}$$

$$\varepsilon_y = \frac{1}{E_p}[\sigma_y - \nu_p(\sigma_z + \sigma_x)] \tag{23}$$

$$\varepsilon_z = \frac{1}{E_p}[\sigma_z - \nu_p(\sigma_x + \sigma_y)] \tag{24}$$

The calculated effective modulus is 3.92GPa for hydrostatic compression (assuming the Poisson's ratio 0.25). While the effective modulus is 1.46GPa and Poisson's ratio is 0.289 for uniaxial compression. We can see the modulus is much smaller than that of solid materials (70GPa).

4. Summary

A 3D numerical model has been developed for the estimation of the effective thermal and mechanical properties of particle bed materials. The model is able to follow the rearrangement of the particles under external and internal loads. Loading processes are given as series of load steps while an iteration method is used to find the equilibrated, compatible and physically correct state of the assembly for each load step. Preliminary calculations confirmed that the effective modulus of particulate material has a much lower magnitude than that of the solid material in addition to being packing and stress dependent.

References

[1] Ying, Alice, Zi Lu and M. A. Abdou, "Mechanical Behavior and Properties of Solid Breeder Blanket Packed Beds," presented at ISFNT-4, Tokyo, Japan, April (1997). To be published in Fusion Engineering & Design.

[2] M. A. Abdou, Ying, Alice, and Zi Lu, "Numerical Derivation of Thermal and Mechanical Properties of Ceramic Blanket Particle Bed Materials," presented at ICFRM-8, Sendai, Japan, October (1997). To be published in Journal of Nuclear Materials.

[3] Ying, Alice and M. A. Abdou, "Analysis of Thermomechanical Interactions and Properties of Ceramic Breeder Blankets," presented at ISFNT-4, Tokyo, Japan, April (1997). To be published in Fusion Engineering & Design.

[4] Cundall, P.A. and O.D.L. Strack (1979), A discrete numerical model for granular assembilies, Geotechnique 29 (1), 47-65.

[5] Cundall, P.A. (1988), Computer simulation of dense sphere assemblies, in: M Satake and J.T. Jenkins, eds., Micro-mechanics of Granular Materials, (Proc. US/Japan Seminar, October 26-30, 1987), Elseview, Amsterdam, pp. 113-123.

[6] Kishino, Y. (1988), Disc model analysis of granular media, in: M. Satake and J.T. Jenkins, eds., Micromechanics of Granular Materials, Elsevier, Amsterdam, pp. 143-152.

[7] Serrano, P.A. and J.M. Rodiriguez-Ortiz (1973), A contribution to the mechanics of heterogenerous granular media, Proc. Symp. Placticity and Soil Mechanics, Cambridge, pp. 215-228.

[8] Johnson, K.L. (1985), Contact Mechanics, Cambridge University Press, London.

[9] Mindlin, R.D. (1949), Compliance of elastic bodies in contact, Journal of Applied Mechanics, Vol. 16, 259

[10] Mindlin, R.D. and Deresiewicz, H. (1953), Elastic spheres in contact under varying oblique forces, Journal of Applied Mechanics, Vol. 20, 327

[11] Singer, I.L. and Pollock, H.M. (1992), Fundamental of Friction: Macroscopic and Microscopic Processes, Kluwer Academic, Dordrecht, The Netherlands.

[12] Feda, Jaroslav (1982), Mechanics of Particulate Materials - The principles, Elsevier, New York.